J Mater Sci (2009) 44:3020–3025
DOI 10.1007/s10853-009-3398-7

Preparation and electrochemical behavior of methylene blue intercalated into layered niobate $K_4Nb_6O_{17}$

Xiaobo Zhang · Dongsheng Feng · Meifeng Chen · Zhidan Ding · Zhiwei Tong

Received: 25 September 2008 / Accepted: 16 March 2009 / Published online: 2 April 2009

Abstract $K_4Nb_6O_{17}$ nano-layered compound was obtained by solid-phase synthesis and then methylene blue (MB) was intercalated into layered niobate $K_4Nb_6O_{17}$ interlayer I by a two-step guest-guest exchange method using the intercalation compound, methyl viologen (MV^{2+})–$K_4Nb_6O_{17}$, as precursor. The optically transparent MB^+–$K_4Nb_6O_{17}$ nanocomposite thin film has been characterized by XRD, IR, TGA, elemental analysis, UV, and electrochemical measurements. It was estimated that the intercalated MB^+ ions are mainly aggregated. The cyclic voltammogram of the MB^+–$K_4Nb_6O_{17}$ nanocomposite thin film exhibited a fine diffusion-controlled cathodic process, which hints the possibility of being utilized as an electrode modifying material.

Introduction

Nanostructured layered metal oxides are a kind of amazing materials with unique two-dimensional structure. Structural, textural, and compositional modifications of layered metal oxides have been investigated to develop new materials with tailored properties, such as catalysis [1], photocatalysis [2–4], electrooxidation [5] and photoluminescent behaviors [6, 7], etc. $K_4Nb_6O_{17} \cdot 3H_2O$ is a unique semiconductor material possessing two alternative interlayer spaces (interlayer I and II) formed by $[Nb_6O_{17}]^-$ layers, between which hydrated and non-hydrated K^+ ions exist to maintain the charge balance [8, 9]. The hydrated K^+ ions in interlayer I can be directly exchanged by both monovalent and multivalent ions [10, 11], as is shown in Fig. 1. Intercalation reactions of $K_4Nb_6O_{17}$ with metal ions [12, 13], methylviologen [10, 14–17], $[Ru(phen)_3]^{2+}$ ions [18], $[Ru(bpy)_3]^{2+}$ [19–23], rhodamine 6G (R6G) dye [24], porphyrin [25, 26] have been achieved, the photocatalytic, photoelectrochemical, and photo-induced electron-transfer behaviors of the intercalation nanocompound have been extensively investigated. However, although the electrochemical behaviors of the intercalated ions have been studied, the prospective utilization of the nanocomposites as modified electrodes is not widely discussed.

Methylene blue (MB) is a kind of basic dye with plane structure (Fig. 2), which is widely used for electrochemical applications, such as catalyst-mediator in electrochemical biosensors. To overcome the water-soluble disadvantages, MB has been immobilized in various matrices such as silicate [27], barium phosphate [28], TiO_2 [29], mordenite-type zeolite [30], zirconium phosphate [31], layered manganese oxide [32]. MB^+ intercalated $K_4Nb_6O_{17}$ has been synthesized by ion-exchange [33] and electrostatic self-assembly deposition (ESD) [34] method, but the electrochemical behavior of intercalated MB^+ was not reported in detail.

In the present work, MB was intercalated into interlayer I of $K_4Nb_6O_{17}$ by host–guest ion exchange method by use of layered MV^{2+}–$K_4Nb_6O_{17}$ as precursor. The MB^+–$K_4Nb_6O_{17}$ nanocomposite was characterized by X-ray diffraction, IR, TGA, elemental analysis, and UV spectroscopy. The electrochemical behaviors of the MB^+–$K_4Nb_6O_{17}$ hybrid thin film electrode were studied.

X. Zhang · D. Feng · M. Chen · Z. Ding · Z. Tong (✉)
Department of Chemical Engineering, Huaihai Institute of Technology, Lianyungang 222005, People's Republic of China
e-mail: zhiweitong575@hotmail.com

Z. Tong
SORST, Japan Science and Technology Agency (JST), Kawaguchi Center Building 4-1-8, Kawaguchi-shi, Saitama 332-0012, Japan

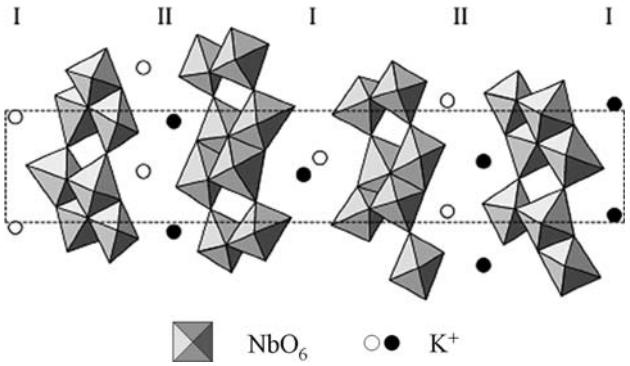

Fig. 1 The structural model of $K_4Nb_6O_{17} \cdot 3H_2O$ showing two different interlayers

Experimental

Analytical Nb_2O_5 and KOH were purchased from Sinopharm Chemical Reagent Co., Ltd., methylviologen chloride and methylene blue were purchased from Tokyo Kasei, all reagents were used without further purification.

The layered compound, $K_4Nb_6O_{17} \cdot 3H_2O$, employed here was prepared by calcination of a 2.1:3.0 molar mixture of K_2CO_3 and Nb_2O_5 at 1100 °C for 10 h, according to the procedures reported by Nassau et al. [35]. Figure 1 shows the layered structure of $K_4Nb_6O_{17} \cdot 3H_2O$. $K_4Nb_6O_{17}$ consists of octahedral units of NbO_6, which form a two-dimensional layered structure via bridging oxygen atoms. The layers are negatively charged, and K^+ ions exist between the layers to compensate for the negative charges of the layers.

The intercalation compound of $K_4Nb_6O_{17}$ with MB^+ is generally very difficult to prepare by a direct reaction because of the bulkiness of MB^+. A two-step intercalation was thus attempted by adopting methylviologen-$K_4Nb_6O_{17}$ intercalation compounds as the intermediate. The methylviologen cation (MV^{2+}) can be smoothly intercalated into interlayer I of $K_4Nb_6O_{17}$. [10, 14–17] The nanostructured hybrid MV^{2+}–$K_4Nb_6O_{17}$ was prepared by treating $K_4Nb_6O_{17} \cdot 3H_2O$ with an aqueous solution of excess methylviologen chloride and then allowing it to stand for 3 weeks at 70 °C. The resultant product was washed with deionized water until the MV^{2+} absorption could not be detected at 257 nm in the filtrate solution [22].

To make the MB^+–$K_4Nb_6O_{17}$ hybrid film, 150 μL aqueous suspension of MV^{2+}–$K_4Nb_6O_{17}$ composite was cast onto a quartz glass plate (20 × 40 mm^2) to obtain an optically transparent film, and then the plate was placed in a 5 mM aqueous solution of methylene blue for 2 weeks. Rinsed the plate with deionized water carefully and dried to obtain a dark blue MB^+–$K_4Nb_6O_{17}$ nanocomposite thin film. All the procedures were prepared at room temperature. A thin film of MB^+–$K_4Nb_6O_{17}$ nanocomposite was prepared on the surface of a glass carbon electrode (GCE) with the same procedure for electrochemical investigation.

XRD patterns of the MV^{2+}–$K_4Nb_6O_{17}$ and MB^+–$K_4Nb_6O_{17}$ hybrid were collected with a M21X (MAC Co., Ltd.) diffractometer with monochromatic Cu Kα radiation ($\lambda = 0.15406$ nm) with 2θ going from 1.5° to 40° in 1° steps. UV absorption spectra of the two hybrids were carried out using a UV–vis spectrometer (UV-2550). IR spectra were measured on a WGH-30/6 double-beam IR-spectrometer with the use of KBr pellets. Thermal gravimetric analysis (TGA) was carried out on a Shimadzu DTG-60 apparatus at a heating rate of 20 °C min^{-1} from room temperature to 750 °C in air. Elemental analysis (EA) was performed using a Perkin Elmer 2400-CHN elemental analyzer.

The electrochemical experiments were carried out in a conventional three-electrode electrochemical cell at room temperature, with a platinum electrode as the counter electrode and a saturated calomel electrode (SCE) as the reference electrode. The MB^+–$K_4Nb_6O_{17}$ nanocomposite thin film modified GC electrode was used as the working electrode. The acting electrolyte was 0.1 mol L^{-1} HCl solution. The solution was bubbled with N_2 for 20 min before examination in order to avoid the influence of oxygen. CV scans were carried out on a CHI600b electrochemical workstation at scan rate of 10–500 mV s^{-1}.

Results and discussion

Characterization of MB^+–$K_4Nb_6O_{17}$ nanocomposite

$K_4Nb_6O_{17} \cdot 3H_2O$ was identified by powder X-ray diffraction analysis (Fig. 3a). Sharp peaks indicated the high crystallinity of the $K_4Nb_6O_{17} \cdot 3H_2O$. The d_{020} value is

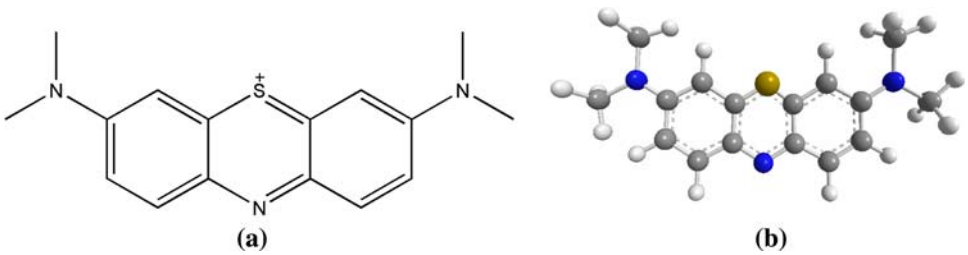

Fig. 2 The molecular structure (**a**) and structural model (**b**) of methylene blue cation

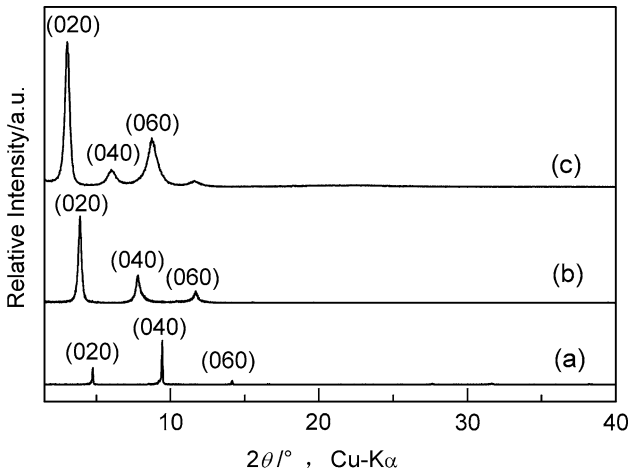

Fig. 3 The X-ray diffraction patterns of **a** $K_4Nb_6O_{17} \cdot 3H_2O$, **b** MV^{2+}–$K_4Nb_6O_{17}$ thin film, and **c** MB^{+}–$K_4Nb_6O_{17}$ thin film

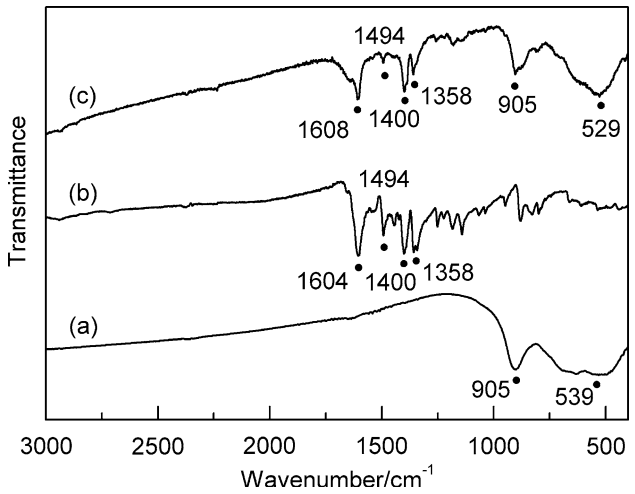

Fig. 5 IR spectra of **a** $K_4Nb_6O_{17}$ **b** MB, and **c** MB^{+}–$K_4Nb_6O_{17}$ nanocomposite

regarded as basal spacing corresponding to the sum of the two adjacent interlayer spaces. The XRD pattern of hydrated potassium niobate $K_4Nb_6O_{17} \cdot 3H_2O$ (Fig. 3a) exhibited a (020) weak diffraction peak at 1.88 nm and an intense peak (040) at 0.94 nm, indicating that water molecules are intercalated only into the interlayer I [18]. The basal spacing of MV^{2+}–$K_4Nb_6O_{17}$ (Fig. 3b, 2.26 nm) was larger than that of $K_4Nb_6O_{17} \cdot 3H_2O$, indicating the substituent of MV^{2+} cations for water molecular in interlayer I. The interlayer I expansion of MV^{2+}–$K_4Nb_6O_{17}$ was calculated as 1.03 nm by subtracting the sum of thickness of the interlayer II and niobate layer of $K_4Nb_6O_{17} \cdot 3H_2O$ (1.23 nm) from the observed basal spacing (2.26 nm) [12].

As was shown in Fig. 3c, the 2θ angle of the (020) diffraction peak of MB^{+}–$K_4Nb_6O_{17}$ was smaller than that of the mediate MV^{2+}–$K_4Nb_6O_{17}$, showing that the intercalation of MB^{+} enlarged the interlayer I spacing of $K_4Nb_6O_{17}$. The interlayer I spacing of MB^{+}–$K_4Nb_6O_{17}$ was calculated as 1.71 nm, which is larger than the spacing of MV^{2+}–$K_4Nb_6O_{17}$ deposited from ESD precipitations [34]. Considering the rectangular dimensions of MB molecular ($1.70 \times 0.76 \times 0.325$ nm^3) [36], we estimate that MB^{+} cations are placed in interlayer I in two ways, which is shown in Fig. 4. The MB^{+} cations may form a double layer parallel to the $[Nb_6O_{17}]^{4-}$ layers, or a single layer standing vertically to the $[Nb_6O_{17}]^{4-}$ layers.

The intercalation of MB into of $K_4Nb_6O_{17}$ was confirmed by IR spectra in Fig. 5. Characteristic infrared absorption peaks of MB [27, 29, 37] in Fig. 5b at 1604 cm^{-1} and 1494 (stretching modes of the aromatic rings), 1400 cm^{-1} (C–N symmetric stretch), 1358 cm^{-1} (–CH_3 symmetric deformation), and of $K_4Nb_6O_{17}$ [38, 39] at 905 cm^{-1} and 539 cm^{-1} (Nb–O stretching vibration) in Fig. 4a appeared in the IR spectrum of MB^{+}–$K_4Nb_6O_{17}$ (Fig. 5c). This confirms that MB has been intercalated into the interlayer spaces of niobate successfully without disturbing the structure of MB. However, there were some differences between the IR spectra of MB^{+}–$K_4Nb_6O_{17}$ and the spectra of MB and $K_4Nb_6O_{17}$. For MB, the adsorption band at 1604 cm^{-1} shifted to 1608 cm^{-1} in the IR adsorption of the nanocomposites, for $K_4Nb_6O_{17}$, the adsorption band at 539 cm^{-1} shifted to 529 cm^{-1}. It can be contributed to the bonding interaction between the Nb–O groups of the niobate and the nitrogen of the aromatic ring of MB [27, 38].

On the base of the elemental analysis data (C = 10.17%, H = 1.38%, N = 2.25%), the molecular formula of the MB^{+}–$K_4Nb_6O_{17}$ nanocomposite is assigned as $MB_{0.63}$–$K_{3.37}Nb_6O_{17} \cdot 2.55H_2O$. The C/N mole ratio of the CHN analysis is calculated as 5.27, which is in good agreement with the observed value, 5.33, proves that the methylviologen ions in the niobate interlayer were replaced by MB^{+}. Figure 6 gives the TG curve of the

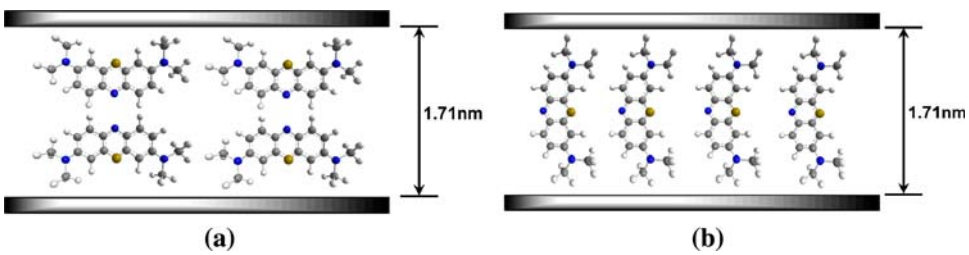

Fig. 4 The proposed intercalation model of MB^{+}–$K_4Nb_6O_{17}$: **a** double layer parallel to $[Nb_6O_{17}]^{4-}$ layers, **b** single layer vertical to $[Nb_6O_{17}]^{4-}$ layers

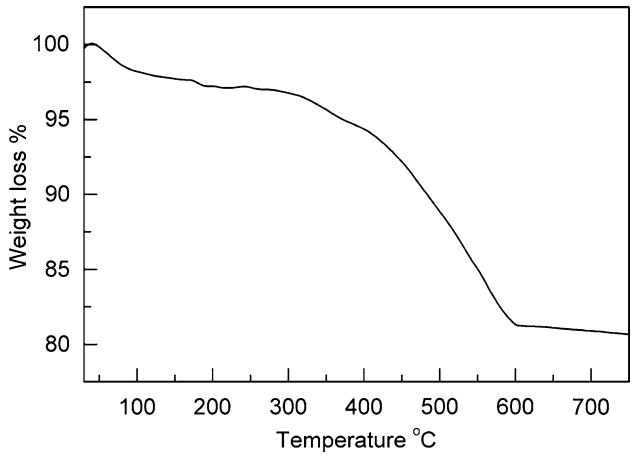

Fig. 6 TGA curve of MB^+–$K_4Nb_6O_{17}$ nanocomposite

MB^+–$K_4Nb_6O_{17}$ nanocomposite. We explained the thermal behavior of the MB^+–$K_4Nb_6O_{17}$ nanocomposite with a two-step weight loss process. The first weight loss step from room temperature to 330 °C is caused by the release of intercalated water, which is dependent on the ambient conditions because of the sensitivity of $K_4Nb_6O_{17}$ to the atmospheric humidity [25, 26]. The second weight loss above 330 °C is due to the decomposition of the organic portion in the nanocomposite interlayer. The total weight loss (19%) is consistent with the sum of the water and MB^+ content determined by the elemental analysis.

The charge density of the $[Nb_6O_{17}]^{4-}$ layer is 0.126 nm^2 per negative charge [16], so the projected area of each MB^+ ion in interlayer I can be calculated as $0.126 \times 2/0.63 = 0.4$ nm^2. Judging from the dimensions of MB molecular, it can be concluded that the intercalation models in Fig. 4 (double layer parallel/monolayer perpendicular) are reasonable.

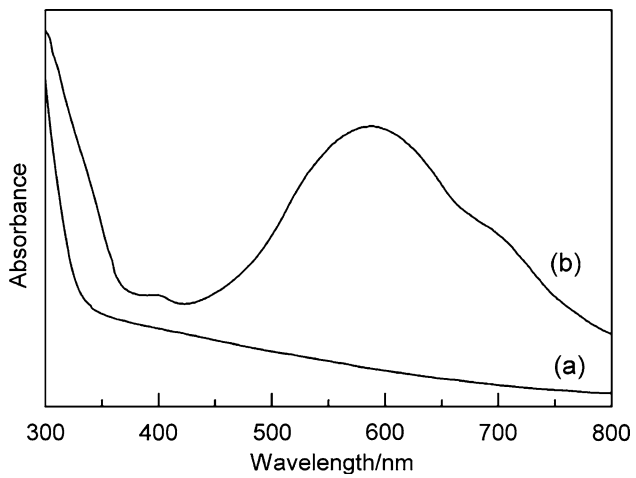

Fig. 7 UV spectrum of MV^{2+}–$K_4Nb_6O_{17}$ (**a**) and MB^+–$K_4Nb_6O_{17}$ (**b**) nanocomposites

UV–vis optical absorption of MB^+–$K_4Nb_6O_{17}$ nanocomposite is shown in Fig. 7b, the UV spectrum of MV^{2+}–$K_4Nb_6O_{17}$ mediate (Fig. 7a) is also given for comparison. There is a broad absorption band in the visible light region in curve b, presenting a maximum absorbance at 586 nm and a shoulder at 680 nm, which confirms the presence of MB^+ in interlayer I of $K_4Nb_6O_{17}$. It is known that MB^+ has strong tendency to aggregate in aqueous solution, the typical maximum absorbance peaks locate at around 665 nm and 610 nm, ascribing to monomer and dimer, respectively [27, 40–44]. The shift of the MB monomer (665 nm) peak toward shorter wavelength clearly denotes that MB^+ cations in $K_4Nb_6O_{17}$ interlayer are aggregated. Considering the position of the maximum (586 nm) and the shape of the signal, we suggest that MB is mainly present as trimers and dimers, while the proportion of monomers is relatively low [36, 45]. This result is corresponding to the MB^+–$K_4Nb_6O_{17}$ nanocomposite obtained by ESD [34].

Electrochemical behavior of MB^+–$K_4Nb_6O_{17}$ nanocomposite thin film

The CV curve of MB in aqueous solution at 50mV s^{-1} scan rate is shown in Fig. 8a. There are a couple of sensitive oxidation/reduction peaks with redox potentials at 0.205 V and 0.174 V, with the midpoint potential $[E_m = (E_{pa} + E_{pc})/2]$ of 0.190 V. The peak separation $[\Delta E_p = (E_{pa} - E_{pc})]$ is 31 mV, which is between the ΔE_p value of individual electron transfer reaction (59 mV) and two-electron transfer reaction (28.5 mV), indicating a two-step individual electron transfer reactions of MB dimer [46, 47].

The cyclic voltammogram of MB^+–$K_4Nb_6O_{17}$ nanocomposite thin film on GCE is shown in Fig. 8b. The redox

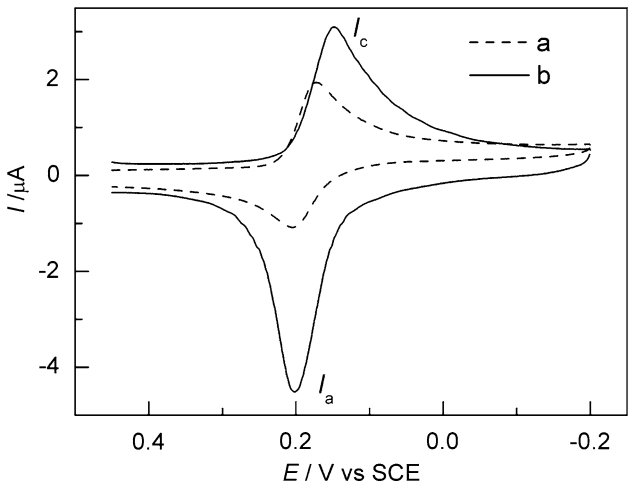

Fig. 8 Cyclic voltammograms of **a** MB (0.05 mmol L^{-1}) and **b** MB^+–$K_4Nb_6O_{17}$ thin film in 0.1 mol L^{-1}HCl solution, scan rate: 50 mV s^{-1}

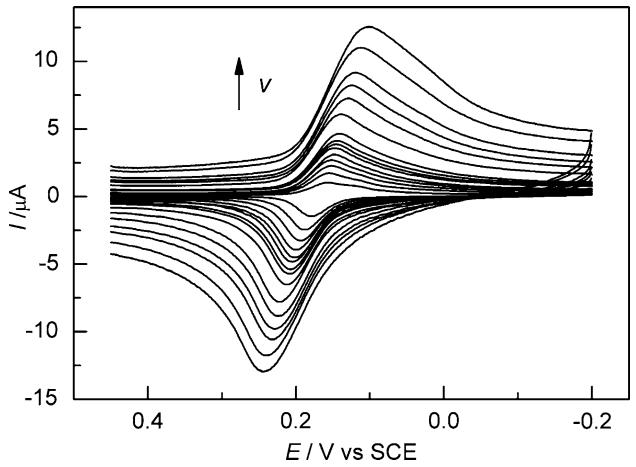

Fig. 9 CVs of MB^+–$K_4Nb_6O_{17}$ thin film at different scan rates (10, 20, 30, 40, 50, 60, 70, 80, 100, 150, 200, 250, 300, 400, 500 mV s^{-1} from inner to outer)

potentials at 0.202 V and 0.148 V with a midpoint potential of 0.175 V are similar with the peaks of MB in solution except the larger peak separation of 54 mV. There is a shift of E_{pc} to more negative values and a shift of E_{pa} to more positive values with increasing the scan rate (Fig. 9). We describe this redox peaks as a two-electron quasi-reversible redox process of MB dimer [31, 48–50]. The linear dependence of the cathodic peak current (I_c) on the square root of the scan rate (Fig. 10) displays a planar diffusion controlled reduction behavior of MB^+ cations in niobate interlayer. The ΔE_p increased from 22 mV up to 143 mV when the scan rate varied from 10 to 500mV s^{-1}, indicating a slow electron diffusion process of the MB^+ cations in the interlayer space at high scan rates. This is due to the semiconducting nature of the niobate matrix [31].

The ideal linear relationship in Fig. 10 indicates a fine mass transfer process, which is suitable for utilization as

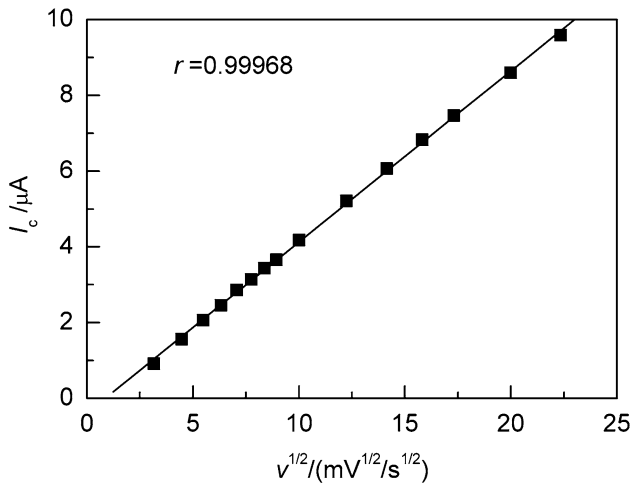

Fig. 10 $I_c \sim \upsilon^{1/2}$ curve for MB^+–$K_4Nb_6O_{17}$ layer nanocomposite thin film in 0.1 mol L^{-1} HCl solution

electrode modifying. In order to test the electrochemical stability of the MB^+–$K_4Nb_6O_{17}$ hybrid film, the modified GCE was tested again after exposure in air for 7 days. The cathodic and anodic currents of redox peaks I were still 90% of initial value at almost the same peak potential, confirming the good immobilization of MB in niobate interlayer spacings.

Conclusion

Laminar nanomaterial $K_4Nb_6O_{17}$ was synthesized through solid-phase synthesis and characterized by XRD. Methylviologen was intercalated into interlayer I of $K_4Nb_6O_{17}$ by ion exchange reaction. Then methylene blue (MB) substituted the MV^{2+} cations through guest–guest ion exchange method. The two hybrid nanocomposites were characterized using IR, UV, XRD. UV pattern of MB^+/$K_4Nb_6O_{17}$ thin film indicated that the intercalated MB^+ existed mainly as dimer and trimer, while the portion of monomer is fairly low. The cyclic voltammogram of the MB^+–$K_4Nb_6O_{17}$ nanocomposite film exhibited a pair of distinct reductive and oxidative peaks, representing a two-electron redox process of MB dimer. The cathodic current exhibited a fine diffusion-controlled process, and the electrochemical stability of the hybrid film was also proved. We predict that novel MB^+–$K_4Nb_6O_{17}$ nanocomposite has possibility to be used as electrode modifying material.

Acknowledgements This work was supported by a Grant-in-aid for Scientific Research from the Japan Society for the Promotion of Science (JSPS) and the CREST program of the Japan Science and Technology Agency (JST). We are grateful to young and middle aged academic leaders of Jiangsu Province universities' "blue and green blue project." This work is also be supported by National Natural Science Foundation of China (Grant No. 50873042).

References

1. Centi G, Perathoner S (2008) Microporous Mesoporous Mater 107:3
2. Schottenfeld JA, Benesi AJ, Stephens PW, Chen GG, Eklund PC, Mallouk TE (2005) J Solid State Chem 178:2313
3. Machida M, Ma XW, Taniguchi H, Yabunaka J, Kijima T (2000) J Mol Cat A Chem 155:131
4. Paek MJ, Kim TW, Hwang SJ (2008) J Phys Chem Solid 69:1444
5. Forti JC, Manzo-Robledo A, Kokoh KB, de Andrade AR, Alonso-Vante N (2006) Electrochim Acta 51:2800
6. Matsumoto Y, Unal U, Kimura Y, Ohashi S, Izawa K (2005) Phys Chem B 109:12748
7. Kudo A, Sakata T (1996) J Phys Chem 100:17323
8. Gasperin M, Le Bihan MT (1980) J Solid State Chem 33:83
9. Gasperin M, Le Bihan MT (1982) J Solid State Chem 43:346
10. Nakato T, Sugahara Y, Kuroda K, Kato C (1991) Mater Res Soc Symp Proc 233:169

11. Mishra SP, Singh VK, Towaro D (1998) Appl Radiat Isot 49:1467
12. Kinomura N, Kumada N, Muto F (1985) J Chem Soc Dalton Trans 2349
13. Nunes LM, de Souza AG, de Farias RF (2001) J Alloys Compd 319:94
14. Nakato T, Kuroda K, Kato C (1989) J Chem Soc Chem Commun 1144
15. Nakato T, Kuroda K, Kato C (1992) Chem Mater 4:128
16. Nakato T, Kuroda K, Kato C (1993) Catal Today 16:471
17. Tong ZW, Takagi S, Shimada T, Tachibana H, Inoue H (2006) J Am Chem Soc 128:684
18. Yao K, Nishimura S, Ma T, Okamoto K, Inoue K, Abe E, Tateyama H, Yamagishi A (2001) J Electroanal Chem 510:144
19. Nakato T, Kusunoki K, Yoshizawa K, Kuroda K, Kaneko M (1995) J Phys Chem 99:17896
20. Furube A, Shiozawa T, Ishikawa A, Wada A, Domen K, Hirose C (2002) J Phys Chem B 106:3065
21. Yao K, Nishimura S, Imai Y, Wang HZ, Ma TL, Abe E, Tateyama H, Yamagishi A (2003) Langmuir 19:321
22. Tong ZW, Takagi S, Tachibana H, Takagi K, Inoue H (2005) J Phys Chem B 109:21612
23. Tong ZW, Takagi S, Tachibana H, Takagi K, Inoue H (2005) Chem Lett 34:608
24. Shinozaki R, Nakato T (2004) Langmuir 20:7583
25. Bizeto MA, Constantino VRL (2005) Microporous Mesoporous Mater 83:212
26. Bizeto MA, de Faria DLA, Constantino VRL (2002) J Mater Sci 37:265. doi:10.1023/A:1013687825874
27. Yao H, Li N, Xu S, Xu JZ, Zhu JJ, Chen HY (2005) Biosens Bioelectron 21:372
28. Lazarin AM, Airoldi C (2004) Anal Chim Acta 523:89
29. David GT, Xavier D, Nieves CP, José AA (2007) J Photochem Photobiol A Chem 187:45
30. Arvand M, Sohrabnezhad Sh, Mousavi MF, Shamsipur M, Zanjanchi MA (2003) Anal Chim Acta 491:193
31. Dilgin Y, Dursun Z, Nisli G, Gorton L (2005) Anal Chim Acta 542:162
32. Yang XS, Chen X, Zhang X, Yang WS, Evans DG (2008) Sens Actuators B 129:784
33. Kaito R, Kuroda K, Ogawa M (2003) J Phys Chem B 107:4043
34. Unal U, Matsumoto Y, Tamoto N, Koinuma M, Machida M, Izawa K (2006) J Solid State Chem 179:33
35. Nasssu K, Shiever WJ, Bernstein LJ (1969) J Electrochem Soc 116:348
36. Klika Z, Čapková P, Horáková P, Valášková M, Malý P, Macháň R, Pospíšil M (2007) J Colloid Interface Sci 311:14
37. Yan Y, Zhang M, Gong K, Su L, Guo Z, Mao L (2005) Chem Mater 17:3457
38. Jehng JM, Wachs IE (1991) Chem Mater 3:100
39. Guo X, Hou W, Bao G, Yan Q (2006) Solid State Ionics 177:1293
40. Ghanadzadeh A, Zeini A, Kashef A, Moghadam M (2008) J Mol Liq 138:100
41. Guo RG, Fan GK, Liu TQ (2000) Acta Chim Sin 58:636
42. Ramasamy V, Anandalakshmi K (2008) Spectrochim Acta A 70:25
43. He XW, Feng XZ, Shen HX (1995) J Anal Sci 11:1
44. Galagan Y, Su WF (2008) J Photochem Photobiol A Chem 195:378
45. Fergus G, Carla CS, Miguel GN (1994) Langmuir 10:3749
46. Žutić V, Svetličić V, Lovrić M, Ružić I, Chevalet J (1984) J Electroanal Chem 177:253
47. de Araujo Nicolai SH, Rodrigues PRP, Agostinho SML, Rubim JC (2002) J Electroanal Chem 527:103
48. Liao F, Zhu QT, He XY, Ai Z, Cai DC (2007) Chem Rev Appl 19
49. Xian YZ, Liu F, Xian Y, Zhou YY, Jin LT (2006) Electrochim Acta 51:6527
50. Chen HY, Ju HX, Xun YG (1994) Anal Chem 66:4538